

RADIAL VELOCITY DISTRIBUTION AND LINE STRENGTHS OF 33 CARBON STARS
IN THE GALACTIC BULGENEIL D. TYSON¹ AND R. MICHAEL RICH^{1,2}

Department of Astronomy, Columbia University

Received 1990 July 6; accepted 1990 July 30

ABSTRACT

We report radial velocities and spectroscopy for the 33 carbon stars discovered by Azzopardi, Lequeux, and Rebeiro in low-extinction windows to the Galactic bulge along $l = 0^\circ$. We find the velocity dispersion to be $113 \pm 14 \text{ km s}^{-1}$ and the mean to be $-44 \pm 20 \text{ km s}^{-1}$, consistent with the kinematics of bulge K and M giants. The bulge carbon stars have several properties in common with classical early R stars: nineteen show enhanced ^{13}C , and all 33 are too faint to be on the AGB ($M_{\text{bol}} > -2.5$). In contrast to local early R stars and CH stars in $\omega \text{ Cen}$, however, the bulge carbon stars have much stronger NaD and CN absorption. This absorption exhibits a gradient in latitude with the stars with the strongest lines near the Galactic center. We propose that this is caused by a gradient in metallicity which is consistent with what is inferred from bulge color-magnitude diagrams and the properties of M giants. If the bulge carbon stars are genuine early R stars, then the inferred high abundance poses further difficulties for current theories of carbon star formation.

Subject headings: galaxies: The Galaxy — radial velocities — stars: carbon

I. INTRODUCTION

The Galactic nuclear bulge is a metal-rich population that contains a wide range of abundances (Whitford and Rich 1983; Rich 1988). Color-magnitude diagrams of stars in the bulge show main-sequence turnoffs that imply an age greater than 5 Gyr (Terndrup 1988). In an old, metal-rich population, the effective temperatures of red giants are cooler at a given luminosity than a corresponding metal-poor population. Consequently, the red giant branch is shifted to cooler temperatures thus forming a large population of late M giants that would otherwise be early M and K giants. Another feature of this old, metal-rich environment is that one would expect M giants to predominate over carbon stars (Renzini and Voli 1981; Scalo and Miller 1981). Indeed, the extensive low dispersion, infrared M giant grism surveys of the bulge by Blanco and Terndrup (1989) (see also Blanco 1986, 1988 and Blanco, McCarthy, and Blanco 1984) discovered only five carbon stars amid 2187 M giants to give a carbon star-to-M giant star ratio of 0.0023. These surveys targeted the prominent infrared absorption bands of CN which easily distinguish carbon stars from M giants.

Current stellar evolution theory proposes that luminous and high mass ($M_{\text{bol}} \leq -6$, $M \geq 3 M_\odot$) carbon stars form when thermal pulses in the helium burning shell of an asymptotic giant branch (AGB) star permits the envelope's convection zone to dredge the ^{12}C product of 3α helium burning (Iben 1975, 1984; Iben and Renzini 1983). It is also found that lower luminosity, low mass, and low metallicity carbon stars ($M_{\text{bol}} \leq -4$, $M \approx 0.7 M_\odot$, $Z \approx 0.001$) may be formed from semi-convection at the envelope-shell boundary that occurs before and during the dredge-up phase to assist the transfer of carbon (Iben and Renzini 1982*a, b*; Iben 1983). These dredging scenarios enhance carbon relative to oxygen which, for stars with low metallicity, will more readily create an envelope with $\text{C/O} > 1$. The excess carbon atoms (over the number required

to form CO with the entire supply of oxygen) form C_2 and CN molecules whose absorption features dominate their optical spectra. Conversely, stars with high metallicity such as those that are common in the Galactic bulge are expected to reach the planetary nebula phase before the moment when $\text{C/O} \geq 1$.

It was therefore a surprise when Azzopardi, Lequeux, and Rebeiro (1985), using a low-dispersion green grism technique, discovered 33 carbon stars in low-extinction windows (from -2.6 to -10°) to the Galactic bulge. The green sensitivity of the grisms readily highlights the prominent C_2 "Swan" absorption features of carbon stars (see also Sanduleak and Philip 1977). To have eluded the Blanco surveys, it was clear that these must be unusual carbon stars. It is now known from infrared photometry that the carbon stars are relatively blue and underluminous (Rich and Tyson 1991; Rich 1989; Azzopardi, Lequeux, and Rebeiro 1988). The most luminous of these have $M_{\text{bol}} > -2.5$, which is 1.5 mag fainter than the minimum luminosity expected for ^{12}C dredging during helium shell flashes. Azzopardi, Lequeux, and Rebeiro (1988) have inferred high abundances for these carbon stars from the comparison of their infrared colors and magnitudes with globular cluster giant branches of known abundances.

To further understand these enigmatic objects, we present new medium dispersion spectroscopy for the entire sample. This allows us to study two critical issues: the velocity dispersion and the stellar line strengths. In § II we discuss the observations and data reduction, in § III we discuss the radial velocities and velocity distribution, and in § IV we discuss the spectral features and their dependence on Galactic latitude. Last, in § V we propose a scenario for the evolution of these bulge carbon stars.

II. OBSERVATIONS

The 33 carbon stars discovered by Azzopardi, Lequeux, and Rebeiro (1985) are in the eight low-extinction bulge windows (Table 1) identified as Sagittarius 1, Baade's window, Galactic window X2, Sagittarius 2, NGC 6558, Galactic window X1, van den Bergh's Window, and Gröningen-Palomar Survey field 3 (hereafter Sgr 1, BW, GWX 2, Sgr 2, N6558, GWX 1,

¹ Visiting Astronomer, Cerro Tololo Inter-American Observatory operated by the Association of Universities for Research in Astronomy, Inc. under contract with the National Science Foundation.

² Guest Investigator, Las Campanas Observatory.

TABLE 1
BULGE WINDOWS

Window	Galactic Latitude	E_{B-V}
Sgr 1	-2.7	0.6 ^a
BW	-4.0	0.49 ^b
GWX 2	-4.8	0.45 ^c
Sgr 2	-5.0	0.43 ^c
N6558	-6.0	0.41 ^c
GWX 1	-6.5	0.38 ^c
VDB	-8.0	0.25 ^d
GP 3	-10.0	0.15 ^c

^a Topaktas 1981.

^b Blanco and Blanco 1985.

^c From fitted E_{B-V} vs. $\text{csc}|b|$ relation in Blanco and Terndrup 1989.

^d van den Bergh and Herbst 1974.

VDB, GP 3). The carbon star spectra were obtained on the 2.5 m du Pont telescope of Las Campanas Observatory with the two-dimensional photon counter ("2D-Frutti"; Sackett and Hiltner 1976) during 6 nights between 1986 June 15 and June 25. Spectra were recorded in 3040 channels from 4290 to 8410 Å with 128 rows perpendicular to the dispersion. Seeing was consistently less than 2". Velocity standards were observed frequently to secure nightly zero-point corrections and to determine internal errors.

To prepare the data for cross correlation with a standard template, the 33 carbon star spectra were reduced using the FIGARO data reduction package written principally by K. Shortridge. The reduction procedure, similar to that used in Rich (1990), is here outlined briefly.

1. All observations were divided by a normalized flat field taken each night to remove the pixel-to-pixel variation in detector sensitivities to wavelength and intensity.

2. The spectrum of an incandescent light shining through seven holes was used to map and correct for the image distortions.

3. There is also a "shear" distortion that alters the correspondence of wavelength to column number across the spatial dimension that is not corrected in step (2). All frames were shear-corrected with low-order polynomials that were fit to bright arc lines.

4. Spectra were sky-subtracted, collapsed to one dimension, and extracted. After some experimenting, we verified that the "optimal extraction" method of K. Horne (1986) was superior (10%–20% higher S/N) to a simple extraction.

5. He-Ne-Ar arc spectra were used to calibrate the wavelength scale. Typically, 25 spectral lines were available which provided the correspondence between column number and wavelength that gave residuals of less than 0.25 Å (18 km s⁻¹ at 6000 Å).

6. The wavelength scale for each frame was rebinned to equal logarithmic intervals, which produces columns of equal velocity units that are appropriate for cross correlation with the velocity standard.

The S/N of all spectra were improved by co-adding up to five multiple observations. Table 2 contains the carbon star IDs, Galactic coordinates, and line strengths of C₂, Na[D₁ + D₂], and CN as measured by an absorption-line fitting routine described in Rich (1986). Finding charts and accurate coordinates will be reported in a separate publication by Azzopardi, Lequeux, and Rebeiro (1991).

III. RADIAL VELOCITIES

We employed the cross-correlation method of Tonry and Davis (1979) to measure radial velocities. The method is successful when the program stars and a suitably chosen template contain similar line features against which a Doppler shift is derived. Four ω Cen CH star standards were observed (BOND, ROA 55, ROA 70, and ROA 153; Bond 1975 and Wing and Stock 1973), along with two local early R stars (BD + 332399 and HD 90395) analyzed in Dominy (1984). The ω Cen standard ROA 153 (actually a field star) provided the best template match for the program stars. Since all velocities are determined relative to this template we must obtain the radial velocity of ROA 153 independently. The ω Cen standards (including ROA 153) and three of the bulge carbon stars were also observed at high dispersion (0.5 Å resolution) with the CCD red air-Schmidt echelle of the CTIO 4 m telescope on 1989 May 29. Echelle reduction employed software developed by McCarthy (1988) and an additional cross-correlation program written by H. Johnston. A radial velocity of -8.7 ± 0.8 km s⁻¹ for ROA 153 was determined from cross-correlating its echelle spectrum with the radial velocity standard HD 111417 ($V_r = -19.5$ km s⁻¹; Maurice *et al.* 1984). As a secondary verification of the zero point, we measured the separation of the unblended Na D₁ ($\lambda 5995.94$) night sky emission line from the Na D₁ absorption line in the echelle spectrum of the program star Sgr 1-3. This method is independent of the wavelength scale's zero point although it suffers from the assumption that the wavelength centroid for Sgr 1-3's Na D₁ absorption is not skewed by interstellar Na D₁ at different redshifts. We derived $V_{\text{Na D}_1} = 140 \pm 8$ km s⁻¹ which is consistent with $V = 149 \pm 3$ km s⁻¹ determined from cross correlating Sgr 1-3's spectrum with HD 111417.

Nightly zero-point shifts were required to bring the six nights to a common velocity reference. The rms and mean residuals derived from the standards for each night are found in Table 3. Night two required a 56 km s⁻¹ shift, while all other nights required shifts of less than 30 km s⁻¹. Spectra of the standards ROA 55 and ROA 70 were obtained during sub-arcsecond seeing during the beginning of the first and third nights. These conditions rendered the seeing disk smaller than the slit width which produced spurious rms residuals. For nights one and three, we determine the zero-point shifts from the brighter program stars rather than the standards.

Multiple observations (up to five) of each program carbon star were each corrected to the heliocentric system, co-added, and cross-correlated with the template ROA 153. The radial velocities derived for all program stars were then corrected for the -8.7 km s⁻¹ radial velocity of the template standard. Tables 4A and 4B give the heliocentric radial velocity for all individual observations of the standards and the program carbon stars. For the program stars, we derive an internal rms error of 30 km s⁻¹ from the 78 (out of 105) reliable residuals in column (5) of Table 4B. We derive an internal rms error of 26 km s⁻¹ for the standards alone, omitting nights one and three for ROA 55 and ROA 70 (Table 4A). Because final velocities are computed from co-added spectra, the rms velocity residual for the individual observations represents worst case internal errors. The accuracy of a measured velocity is indicated by the height (C_{max}) and symmetry of the peak in the cross-correlation function generated between the spectrum of the template and program stars. A height of 1.0 indicates a perfect match, while a symmetric peak permits reliable centroiding to determine the relative shift in spectral features. Co-added spectra typically

TABLE 2
33 BULGE CARBON STARS

ID (1)	<i>l</i> (2)	<i>b</i> (3)	C_2 (SWAN)		Na ($D_1 + D_2$) (6)	CN		^{13}C (9)	Hz (10)	COMMENTS (11)
			$\Delta v = 0$ (4)	$\Delta v = -1$ (5)		$\nu(3, 0)$ (7)	$\nu(4, 1)$ (8)			
Sgr 1-1	1°34	-2°39	0.73	0.62	4.73	0.39	0.16	Med	Med	
Sgr 1-2	1.28	-2.78	0.90	0.72	6.43	0.39	0.19	Med	Weak	Hd
Sgr 1-3	1.53	-2.65	1.18	0.79	6.99	0.45	0.28	Weak	Weak	Hd
Sgr 1-4	1.65	-2.63	0.97	0.78	6.84	0.49	0.38	Med	Med	
BW-1	1.29	-4.02	0.67	0.64	5.89	0.32	0.19	Med	Weak	Hd
BW-2	1.25	-4.24	0.77	0.64	4.43	0.37	0.23	Str ^a	Weak	J, Hd
BW-3	1.14	-3.66	0.79	0.64	5.91	0.42	0.25	Weak	Med	
BW-4	1.24	-3.61	0.43	0.29	6.33	0.29	0.13	Weak	Weak	Hd
BW-5	1.03	-3.68	0.45	0.41	6.33	0.26	0.05	Weak	Med	
BW-6	0.91	-3.82	0.85	0.68	6.47	0.49	0.31	Med	Weak	Hd
BW-7	1.04	-4.32	0.75	0.63	3.84	0.35	0.23	Str	Weak	J, Hd
BW-8	0.73	-4.12	0.46	0.25	6.45	0.32	0.14	Weak	Weak	Hd
BW-9	0.74	-4.09	0.86	0.73	5.62	0.34	0.21	Weak	Weak	Hd
GWX 2-1	0.86	-4.38	1.02	0.80	7.39	0.48	0.37	Med ^a	Weak	Hd
GWX 2-2	0.34	-4.82	0.42	0.29	4.61	0.31	0.06	Weak	Med	
GWX 2-3	0.70	-4.84	0.31	0.13	5.89	0.37	0.14	Weak:	Med	CS
GWX 2-4	1.04	-4.70	0.42	0.29	3.13	0.22	0.08	Weak	Med	
GWX 2-5	0.66	-5.06	0.36	0.26	2.71	0.26	0.11	Weak	Str	
GWX 2-6	1.05	-4.99	0.67	0.55	4.34	0.31	0.18	Weak	Med	
Sgr 2-1	3.90	-4.86	0.44	0.19	7.19	0.36	0.27	Med	Weak	Hd
Sgr 2-2	4.40	-5.49	0.63	0.39	4.61	0.38	0.29	Med	Weak	Hd
N6558-1	-0.03	-5.97	0.40	0.20	2.60	0.23	0.14	Weak	Str	
N6558-2	0.34	-5.83	0.41	0.27	3.46	0.21	0.17	Med	Str	
N6558-3	0.56	-5.74	0.45	0.25	5.37	0.27	0.18	Str	Str	J
N6558-4	0.37	-5.96	0.68	0.46	4.19	0.31	0.22	Med: ^a	Med	
N6558-5	0.29	-6.21	0.69	0.72	3.25	0.16	0.10	Weak ^a	Med	
N6558-6	0.57	-6.20	0.54	0.40	2.10	0.21	0.12	Str	Str	J
GWX 1-2	-0.34	-6.27	1.15	1.05	3.91	0.40	0.30	Str	Weak	J, Hd
GWX 1-3	-0.36	-6.52	0.50	0.37	4.47	0.33	0.20	Med	Med	
GWX 1-4	-0.09	-6.39	0.23	0.05	8.19	0.18	0.10	Weak	Med	CS
GWX 1-6	-0.05	-6.61	0.41	0.26	4.19	0.33	0.11	Str	Str	J
VDB-1	0.21	-7.99	0.39	0.29	4.40	0.29	0.20	Med:	Med	
G-P 3-1	-0.24	-9.89	0.38	0.25	1.80	0.15	0.09	Med:	Med	

NOTE.—All line strengths computed with "BWID" as described in Rich 1986.

^a Spectrum also featured in Fig. 7 where ^{13}C isotopic shifts are highlighted.

COL. (1).—Carbon star ID given by Azzopardi *et al.* 1985.

COLS. (2) and (3).—Galactic latitude and longitude in degrees.

COL. (4).—Line strength of C_2 ($\Delta v = 0$) in magnitudes.

COL. (5).—Line strength of C_2 ($\Delta v = -1$) in magnitudes.

COL. (6).—Equivalent width of Na D lines in angstroms.

COL. (7).—Line strength of CN(3, 0) in magnitudes.

COL. (8).—Line strength of CN(4, 1) in magnitudes.

COL. (9).—Strength of $^{12}C^{13}C$ compared with $^{12}C^{12}C$ estimated visually. See § IVb for discussion.

COL. (10).—Strength of Hz estimated visually. See § V for discussion.

COL. (11).—J star (^{13}C -rich), Hd star (hydrogen deficient), or CS star (weak C_2) candidates are noted. Until accurate temperatures are available for a more detailed classification, we estimate that all 33 are early R stars (R0–R4).

have $S/N \geq 15$, which consistently generate higher cross-correlation peaks ($0.4 < C_{\max} < 0.9$) than the individual observations ($0.1 < C_{\max} < 0.6$).

As a secondary check on the standards, we also used the brightest program carbon star GWX 2-4 as a velocity template. The derived velocities for the program stars were consistently within 30 km s^{-1} ($\approx 1 \sigma$) of the velocities determined with ROA 153 as the template.

To be in a low-extinction window to the Galactic bulge does not guarantee bulge membership; this must be established kinematically. Figure 1 shows the radial velocity distribution of the 33 carbon stars and the corresponding best-fit normal distribution. The dispersion of the entire sample is $110 \pm 14 \text{ km s}^{-1}$ when corrected for the internal rms errors. The velocity

dispersion for the subset of nine carbon stars in Baade's window ($\sigma_v = 100 \pm 24 \text{ km s}^{-1}$) is consistent with that of the Baade's window K giants ($\sigma_v = 104 \pm 10 \text{ km s}^{-1}$; Rich 1990), and Baade's window M giants ($\sigma_v = 113 \pm 11 \text{ km s}^{-1}$; Mould 1983). The velocity dispersion drops, however, from 131 km s^{-1} for the 11 innermost carbon stars ($|b| < 4^\circ 1$), through 111 km s^{-1} ($4^\circ 1 < |b| < 5^\circ 7$) for the middle 11, to 81 km s^{-1} ($5^\circ 8 < |b| < 9^\circ 9$) for the outer 11 (see Table 5 and Fig. 2). The large velocity dispersions and latitude dependence are consistent with the carbon stars belonging to the bulge population rather than the solar neighborhood. The rapid drop in velocity dispersion with latitude is also shared by 18 RR Lyrae stars in the GP3 bulge window ($b = -10^\circ$); Rodgers (1977) finds $\sigma_v = 62 \pm 10 \text{ km s}^{-1}$ (see Fig. 2).

TABLE 3
NIGHTLY ZERO-POINT SHIFTS

Night (1)	$\langle V_T - V_0 \rangle$ (2)	ϵ (3)	N (4)
1	-28.6 ^a	33.2	4 ^a
2	-56.2	30.0	4
3	-11.5 ^a	17.6	6 ^a
4	+16.8	12.9	5
5	-0.8	19.8	3
6	-14.1	9.2	2

^a Velocity residuals derived from program stars where V_T is assumed to be the velocity derived from co-adds of nights 2, 4, 5, and 6. (See § III for discussion.)

COL. (1).—Night sequence (June 15, 16, 17, 18, 19, 25).

COL. (2).—Mean residual where V_T = velocity for standards (obtained from echelle observations and from Webbink (1981) and V_0 = observed velocity.

COL. (3).—RMS residual.

COL. (4).—Number of standards used.

We do not have enough longitude coverage ($-0^\circ 4 < l < +4^\circ 4$) to test for rotation in the Galactic plane. The mean velocity for the sample, however, is significantly nonzero: $\langle v \rangle = -44 \pm 20 \text{ km s}^{-1}$. It drops from $\langle v \rangle = -10 \pm 39 \text{ km s}^{-1}$ for the inner 11 stars, through $\langle v \rangle = -25 \pm 33 \text{ km s}^{-1}$ for the middle 11 stars, to $\langle v \rangle = -100 \pm 24 \text{ km s}^{-1}$ for the outer 11 (see Table 5). It would, of course, be unwise to develop bulge models on these statistics of 11, particularly since carbon stars may not characterize the bulge population as securely as K and M giants. We note, however, that the mean velocity of 57 M giants in Baade's window ($-10 \pm 19 \text{ km s}^{-1}$; Mould 1983), 88 K giants in Baade's window ($-19 \pm 8 \text{ km s}^{-1}$; Rich 1990), and the 18 RR Lyrae stars in GP 3 ($-42 \pm 15 \text{ km s}^{-1}$; Rodgers 1977) are all negative. Recent bulge models (e.g., Blitz and Spergel 1991 and Gerhard and Vietri 1986) propose some degree of triaxiality for the bulge; it would be interesting to compare the mean velocities of populations in northern bulge latitudes with these of the southern bulge to search for minor axis rotation.

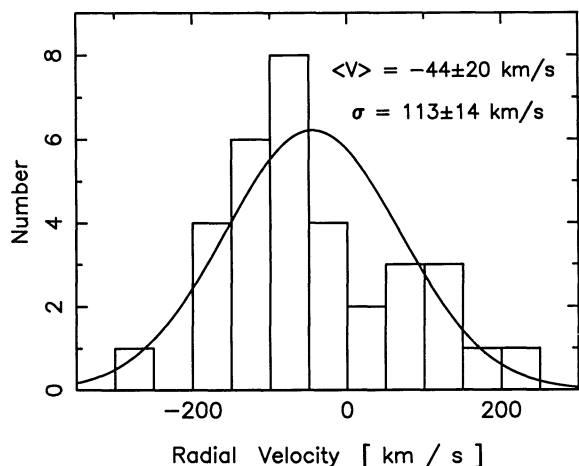


FIG. 1.—Radial velocity distribution histogram together with the best-fitting normal distribution. The dispersion is $113 \pm 14 \text{ km s}^{-1}$ and the mean velocity is $-44 \pm 20 \text{ km s}^{-1}$. The similarity of this velocity dispersion with that of bulge K and M giants suggests these carbon stars are genuine bulge members.

IV. SPECTRA

a) Line Strength Gradient

Isochrone fits to color-magnitude diagrams in bulge windows (van den Bergh and Herbst 1974; Terndrup 1988), and M giant colors and number counts as a function of latitude and longitude (Blanco 1988 Terndrup, Frogel, and Whitford 1990) indicate a metallicity gradient in the bulge with higher metallicity toward the Galactic center. To determine whether line strengths also indicate this trend, we measured the equivalent widths of the Swan C_2 absorption systems at $\lambda 5165$ ($\Delta v = 0$) and $\lambda 5636$ ($\Delta v = -1$), the CN bands at $\lambda 6928$ ($\Delta v = 3$) and $\lambda 7119$ ($\Delta v = 3$), and the prominent $\text{Na}[D_1 + D_2]$. These measurements used the bandpasses listed in Table 6 and may be found in columns (4)–(8) of Table 2.

We find that NaD is strong ($2 < \text{EW} < 8 \text{ \AA}$) for all stars and shows a latitude dependence (Fig. 3a) that cannot be explained entirely by interstellar absorption; four M giants that fell along the slit within $1'$ of the four carbon stars Sgr 1-4, BW-8, BW-9, and N6558-6 (see Fig. 4) showed little or no NaD absorption. If we assume that interstellar sodium absorption is not likely to vary greatly on arc minute scales, then the absence of NaD absorption in the M giant spectra suggests that very little interstellar sodium has contributed to the NaD absorption in the bulge carbon stars. This is true even for Sgr 1-4, which is found in the innermost ($b \approx -2.7'$) of the eight bulge windows in this study. The NaD line strengths are also 3–4 times larger than expected from an interstellar contribution in the various bulge

TABLE 4A
JOURNAL OF OBSERVATIONS—STANDARDS

ID (1)	V_T (km s^{-1}) (2)	Date (1986) (3)	V_{obs} (km s^{-1}) (4)	$(V_T - V_{\text{obs}})$ (km s^{-1}) (5)
ROA 55	220.4 ± 0.2^a	Jun 15	250.5 ^c	-30.1 ^c
		Jun 16	154.1	66.3
		Jun 17	318.0 ^c	-97.6 ^c
		Jun 18	227.0	-6.6
		Jun 19	243.2	-22.9
		Jun 19	195.7	24.6
ROA 70	213.9 ± 4.4^b	Jun 15	191.7 ^c	22.2 ^c
		Jun 17	-2.8 ^c	216.7 ^c
		Jun 18	204.8	9.1
		Jun 19	181.3	32.6
ROA 153	-8.7 ± 0.2^a	Jun 15	12.3	-21.0
		Jun 15	22.2	-30.8
		Jun 16	-38.3	29.7
		Jun 17	-35.4	26.7
		Jun 18	-0.6	-8.1
		Jun 19	-13.4	4.7
Bond	223.1 ± 0.2^a	Jun 19	-21.9	13.2
		Jun 18	222.8	0.2
		Jun 25	188.5	34.6

^a Velocity from CTIO 4 m echelle observations 1989 May 29. Used as " V_T " for standards only.

^b Velocity from Webbink 1981.

^c Possibly spurious velocities from seeing-disk fluctuations during the first part of nights 1 and 3 (1986 Jun 15 and 17). (See § III.)

COL. (1).—Carbon star ID.

COL. (2).—Heliocentric velocity obtained from echelle observations and from Webbink 1981.

COL. (3).—Date of observation.

COL. (4).—Heliocentric velocity derived from cross-correlation of single observation with ROA 153.

COL. (5).—Velocity residuals.

TABLE 4B
JOURNAL OF OBSERVATIONS—PROGRAM STARS

ID (1)	V_T (km s^{-1}) (2)	Date (1986) (3)	V_{obs} (km s^{-1}) (4)	$(V_T - V_{\text{obs}})$ (km s^{-1}) (5)	ID (1)	V_T (km s^{-1}) (2)	Date (1986) (3)	V_{obs} (km s^{-1}) (4)	$(V_T - V_{\text{obs}})$ (km s^{-1}) (5)
Sgr 1-1	-108.9	Jun 17	-76.0:	-32.8:	GWX 2-3	-56.7	Jun 15	-58.1	1.3
		Jun 17	-113.9	5.1			Jun 25	-57.9	1.2
		Jun 25	-121.8	13.0	GWX 2-4	-42.3	Jun 15	-26.8	-15.5
Sgr 1-2	106.8	Jun 17	96.7	10.1			Jun 15	-35.3	-6.9
		Jun 25	154.0	-47.3			Jun 16
Sgr 1-3	126.3	Jun 17	169.3	-43.0			Jun 18	-33.4	-8.9
(Sgr 1-3	149.0 ± 3 ^a)	Jun 17			Jun 18	3.5	-45.7
		Jun 25	97.0	29.2			Jun 25	-81.2	39.0
Sgr 1-4	211.6	Jun 18	219.6	-8.1	GWX 2-5	-142.3	Jun 25	-1.1	-41.1
		Jun 25	192.1	19.5			Jun 16	-134.9 ^d	-7.4 ^d
BW-1	60.7 ^b	Jun 15	75.4	-14.7			Jun 25	-215.7:	73.4:
		Jun 15	106.4	-45.7	GWX 2-6	-183.3	Jun 16	-209.5:	26.2:
		Jun 19	-4.7	65.4			Jun 16	-231.8	48.5
		Jun 25	52.8	7.9			Jun 17	-138.6	-44.7
BW-2	-59.5	Jun 15			Jun 17	-157.7	-25.6
		Jun 15	-57.3:	-2.3:			Jun 25	-186.1	2.8
		Jun 15	-62.3:	2.8:	Sgr 2-1	132.6	Jun 18	149.7	-17.1
		Jun 18	-37.3	-22.2			Jun 25	71.7	60.9
		Jun 25	-86.4	26.8	Sgr 2-2	-69.2	Jun 18	-65.9	-3.3
BW-3	-98.2	Jun 15	-50.7	-47.5			Jun 25	-85.5	16.3
		Jun 15	-99.7	1.4	N6558-1	65.7	Jun 18	67.4	-1.7
		Jun 17	-187.0 ^d	88.8 ^d			Jun 25	57.1	8.6
		Jun 25	-222.1 ^d	123.9 ^d	N6558-2	-58.8:	Jun 18	-31.0:	-27.8:
BW-4	-29.9	Jun 16	-42.4	12.5	(N6558-2	33.2 ± 4 ^a)	Jun 18	-85.3:	26.5:
		Jun 19	-15.1	-14.8			Jun 19
		Jun 25	-47.9	18.0			Jun 25	26.1:	-85.0:
BW-5	-254.2	Jun 16	-260.5	-6.3	N6558-3	21.0	Jun 18	17.6	3.4
		Jun 16			Jun 25	30.8	-9.8
		Jun 19	-252.9	-1.3	N6558-4	-99.9	Jun 18	-96.0	-3.9
		Jun 25	-231.4	-22.8			Jun 25	-114.2	14.3
BW-6	14.0	Jun 17	22.0	-7.9	N6558-5	-193.7	Jun 18	-166.7	-27.0
		Jun 17	29.3	-15.2			Jun 25	-241.7	48.0
		Jun 19	-4.7	18.7	N6558-6	-148.9	Jun 18	-125.8	-23.0
		Jun 25	-6.4	20.4			Jun 25	-212.5:	63.7:
BW-7	84.4	Jun 17	70.8	13.7	GWX 1-2	-43.9	Jun 18	-35.5	-8.4
		Jun 17	108.8	-24.4			Jun 25	-84.0	40.1
		Jun 17	103.0	-18.6	GWX 1-3	-100.9	Jun 18	-84.1	-16.8
		Jun 19	56.6	27.8			Jun 18	-103.3	2.4
		Jun 25	71.8	12.6			Jun 25	-134.8	33.9
BW-8	-79.7	Jun 17	-83.0	3.3	GWX 1-4	-199.0	Jun 19	-243.2	44.2
		Jun 17	-50.8	-29.0			Jun 19	-178.4:	-20.6:
		Jun 25	-131.5	51.8			Jun 19	-179.6	-19.4
BW-9	-53.8	Jun 17			Jun 25	-66.9:	-132.2:
		Jun 17	-69.8:	16.0:	GWX 1-6	-177.0	Jun 19	-183.6	6.5
		Jun 17			Jun 19	-162.0	-15.0
		Jun 19	28.5	-82.3			Jun 25	-180.9	3.8
		Jun 25	-134.9	81.0	VDB-1	-117.3	Jun 16	-67.1	-50.2
GWX 2-1	157.5	Jun 18	153.5	4.0			Jun 16	-84.4	-32.9
		Jun 18	168.1	-10.6			Jun 17	-226.8 ^d	109.4 ^d
		Jun 25	129.2	28.2			Jun 25	-8.8	-108.6
GWX 2-2	-117.4	Jun 16	-168.2:	50.8:	GP 3-1	-23.4:	Jun 18	-29.6:	6.2:
		Jun 16	-112.7:	-4.7:	(GP3-1	-59.3 ± 3 ^a)	Jun 25
		Jun 25	-76.3:	-41.0:					

^a V_T from CTIO 4 m Echelle observations 1989 May 29.

^b Velocities for all program stars obtained from co-added spectra cross-correlated with the standard ROA 153. (See § III.)

^c Unsuccessful cross-correlation. Frame still used in co-add.

^d Possibly spurious velocities from seeing disk fluctuations during first part of nights 1 and 3 (1986 June 15 and 17). (See § III.)

COL. (1).—Carbon star ID. Names assigned by Azzopardi *et al.* 1985.

COL. (2).—Heliocentric velocity derived from cross-correlation of co-added spectra with ROA 153.

COL. (3).—Date of observation.

COL. (4).—Heliocentric velocity derived from cross-correlation of single observation with ROA 153.

COL. (5).—Velocity residuals.

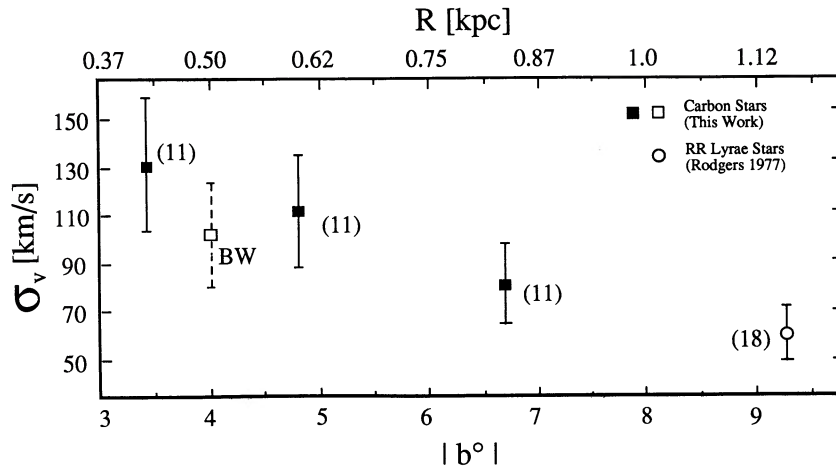


FIG. 2.—Radial velocity dispersion as a function of latitude. The 33 bulge carbon stars were binned into three groups of 11 sorted by increasing Galactic latitude. The points are positioned along the abscissa at the mean latitude for each group. The unfilled square represents the subset of nine carbon stars that are in Baade's window. The unfilled circle represents the velocity dispersion of 18 RR Lyrae stars in GP 3. For reference, the upper border gives the projected physical distance from the Galactic center (with $R_{\odot} = 8$ kpc). Notice that the decline in velocity dispersion for the carbon stars is shared by the RR Lyrae stars.

windows (inferred from a linear dependence on E_{B-V}) based on a 2 \AA interstellar contribution in Baade's window (Rich 1988).

As noted by Scalo (1973), we may expect anomalously strong NaD absorption in stars where $C \approx O$ due to the absence of H_2O and CN opacity, which mimics a higher surface gravity by exposing deeper layers of the atmosphere. We find this effect with the CS stars GWX 1-4 and GWX 2-3. For the rest of the bulge carbon stars, however, the sodium enhancement must have other causes, such as high surface gravity, cool effective temperatures, or high abundance. We cannot rule out the possibility of a latitude gradient in surface gravity or temperature, although there exists no obvious physical mechanism that could lead to such a dependence. For consistency with the bulge M giants, however, we find the simplest interpretation to be an abundance gradient.

The CN $\lambda 6928$ band strength also shows a latitude gradient (Fig. 3b); it follows that NaD and CN $\lambda 6928$ are correlated (Fig. 5). The suspicion that these bulge stars are chemically

unusual is supported by Figure 5, where 25 of the 33 bulge carbon stars define a locus of high NaD and CN line strengths. This locus excludes ROA 153, the ω Cen CH stars (Bond, ROA 55, ROA 70), and local carbon star standards (BD +332399 and HD 90395) of approximately solar Fe abundance (Dominy

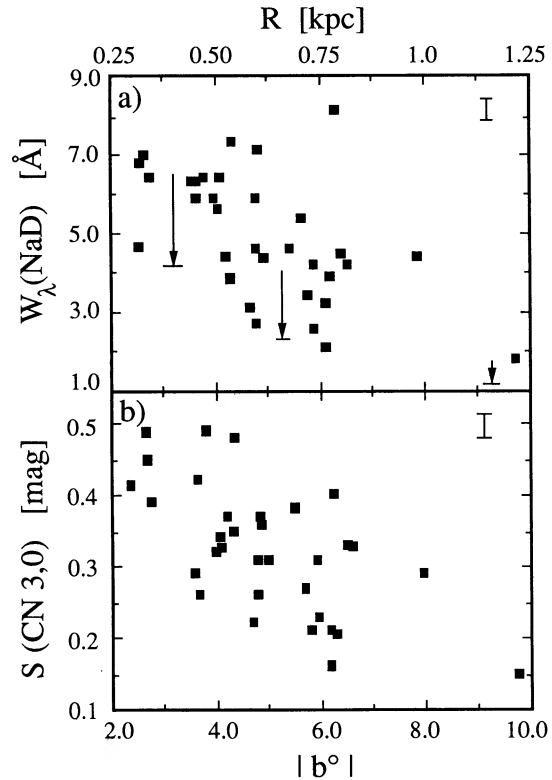


FIG. 3.—(a) NaD equivalent width measured in angstroms as a function of Galactic latitude. The equivalent widths of the NaD lines are 2–3 times larger than can be explained from interstellar absorption. We indicate with arrows (based on measurements in Baade's window of NaD in K giant spectra; Rich 1988) the possible contribution to the equivalent widths assuming a linear dependence on interstellar extinction. (b) CN line strength as a function of latitude measured in magnitudes. The upper scale gives the projected physical distance from the Galactic center (with $R_{\odot} = 8$ kpc).

TABLE 5

BULGE CARBON STAR VELOCITY DISPERSIONS

Sample	Latitude Range $ b $	$\langle V \rangle$ (km s^{-1})	σ_v (km s^{-1})	N
Full sample	2.4–9.9	-44 ± 20	110 ± 14	33
Baade's window	3.6–4.3	-46 ± 33	100 ± 24	9
Inner region	2.4–4.1	-10 ± 39	131 ± 28	11
Middle region	4.2–5.7	-25 ± 33	111 ± 24	11
Outer region	5.8–9.9	-100 ± 24	81 ± 17	11

TABLE 6

REST FRAME BANDPASSES

Species	Blue Continuum (\AA)	Band (\AA)	Red Continuum (\AA)
$C_2 (\Delta v = 0)$	4762–4825	4890–5165	5175–5240
$C_2 (\Delta v = -1)$	5175–5240	5345–5640	5650–5680
$\text{Na}(D_1 + D_2)$	5860–5880	5885–5902	5905–5930
CN (3, 0)	6756–6777	6925–7050	7051–7070
CN (4, 1)	7051–7070	7071–7220	7221–7250

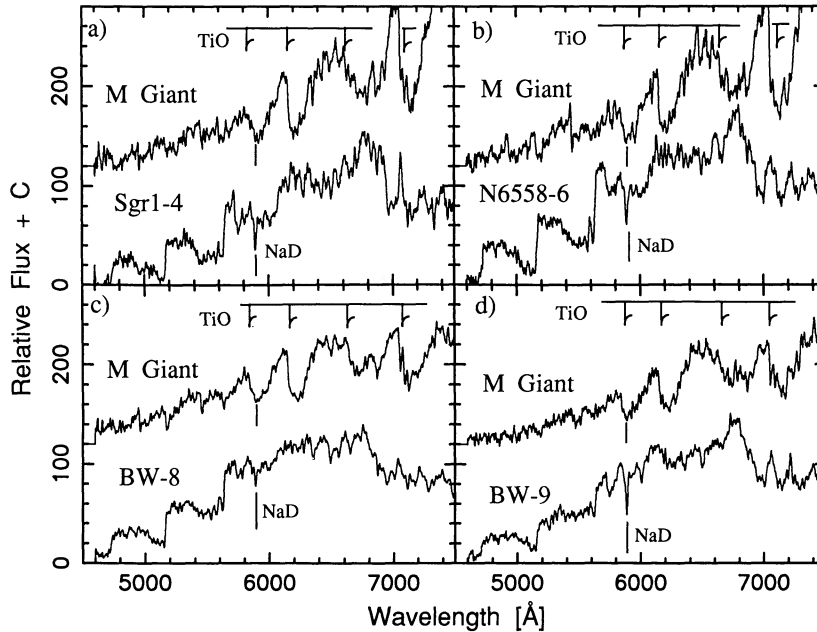


FIG. 4.—(a) Comparison of the carbon star Sgr 1-4 ($b = -2.65$) with an M giant extracted within $1'$ from the same long-slit spectrum. The two stars are thus subject to similar interstellar absorption. Notice the absence of significant NaD absorption ($\lambda 5890, \lambda 5895$) in the M giant's spectrum. We conclude that the NaD is intrinsic to the bulge carbon stars. (b) Same as (a) but for the carbon star N6558-6 ($b = -6.20$). (c) Same as (a) but for the carbon star BW-8 ($b = -4.12$). (d) Same as (a) but for the carbon star BW-9 ($b = -4.09$).

1984). The segregation in Figure 5 suggests two distinct populations: the “normal” early R carbon stars and the high line strength bulge carbon stars. The low line strength subset lies more distant from the Galactic center than Baade's window, although the groups are not fully separated in latitude (see Fig. 6). It is not yet clear whether these stars belong to another low-metallicity population (e.g., the halo), or whether the gap would disappear in a larger sample.

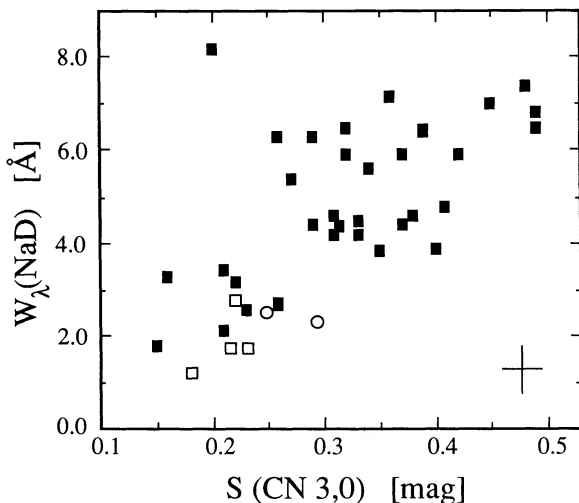


FIG. 5.—NaD correlates with CN. Filled squares are bulge carbon stars. Open squares are ω Cen CH stars and ROA 153. Circles are early R disk carbon star standards with approximately solar Fe abundance (Dominy 1984). Notice that the standards define an isolated area that excludes most of the bulge carbon stars. The bulge carbon star outlier with $W_\lambda(\text{NaD}) \approx 8 \text{ \AA}$ is a CS star.

b) Carbon Isotopes

The interval between 5500 and 6300 Å contains ^{13}C isotope shifts for C_2 and CN. For detail, the region 6080–6300 Å (shifted to rest frame velocities and displayed at 5 Å resolution) is highlighted in Figure 7 for four bulge carbon stars that illustrate the range in prevalence for the $^{12}\text{C}^{13}\text{C}$ bands at $\lambda 6101$ and $\lambda 6168$ when compared with the $^{12}\text{C}^{12}\text{C}$ band heads at $\lambda 6122$ and $\lambda 6191$. Included for comparison is BD +332399, a local carbon star with $^{12}\text{C}/^{13}\text{C} = 5 \pm 4$ from Dominy's (1984) list. The $^{13}\text{C}^{14}\text{N}$ molecular isotope at $\lambda 6259$ is also identified although its strength may not be strongly correlated with $^{12}\text{C}^{13}\text{C}$ (Gordon 1971).

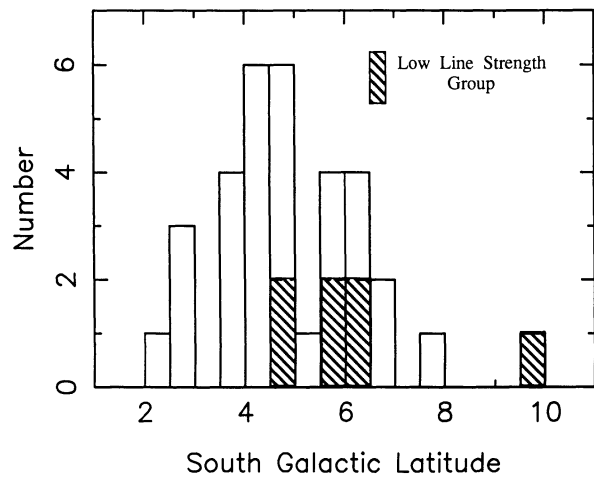


FIG. 6.—Latitude distribution of the 33 bulge carbon stars. The shaded histogram is the set of seven stars that have the smallest NaD and CN line strengths. The low line strength group is farther from the Galactic center than Baade's window at $b \approx -4$ (0.5 kpc).

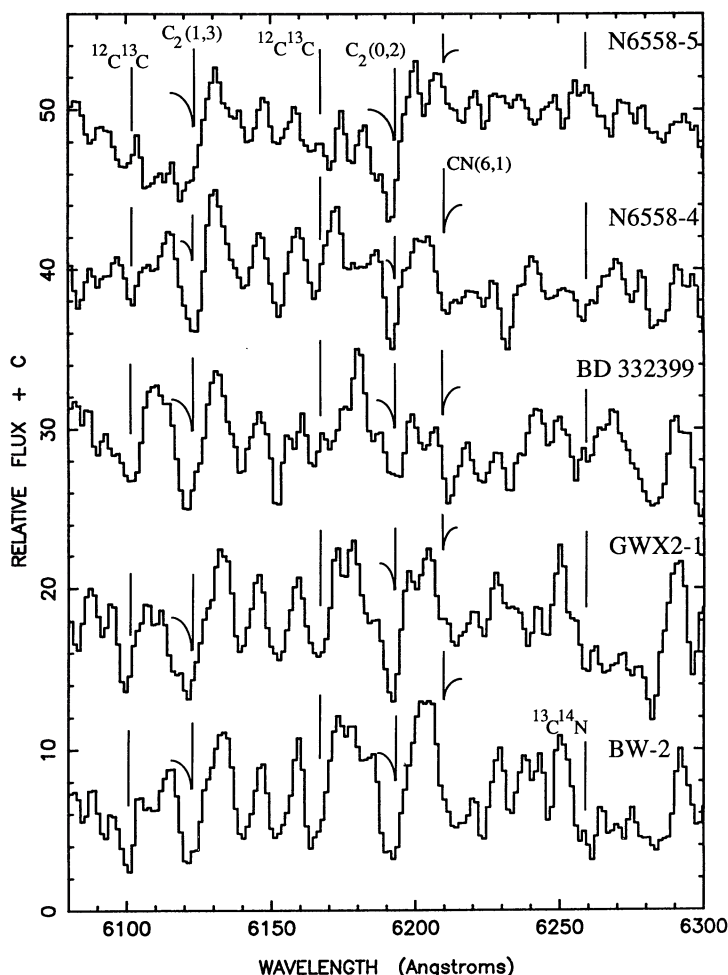


FIG. 7.—Region of the spectrum from 6080 to 6300 Å that highlights isotope shifts for C_2 and CN. Included are four bulge carbon stars (N6558-5, N6558-4, GWX 2-1, BW-2) and one local early R star (BD 332399) from Dominy's (1984) list. The full range of relative absorption strengths between $^{12}C^{13}C$ at $\lambda 6168$ and $^{12}C^{12}C$ at $\lambda 6191$ is displayed. Notice that for N6558-5 the $^{12}C^{13}C$ band head at $\lambda 6168$ is barely visible, whereas for BW-2 the $\lambda 6168$ absorption is strong. The star BD 332399 has been found by Dominy (1984) to have $^{12}C/^{13}C = 5 \pm 4$. Based on this comparison, we suggest that most (19 out of 33) are ^{13}C -rich.

Utsumi (1987) cautions that the low-excitation atomic lines Ca I 3 ($\lambda 6102.7$, $\lambda 6169.1$, $\lambda 6162.2$) coincide with the ^{13}C features and can influence spectral classification at medium resolution, especially in the atomic line-enhanced CS stars. As a secondary check, we classify the ^{13}C strength in these carbon stars from the isotopic band heads of $^{12}C^{13}C$ at $\lambda 5534$, $\lambda 5577$, and $\lambda 5625$ that are shifted from the normal $^{12}C^{12}C$ heads found at $\lambda 5541$, $\lambda 5586$, and $\lambda 5635$. We estimate from visual inspection the presence of $^{12}C^{13}C$ as "weak," "medium," or "strong." Eight stars that would have been classified as "medium" or "strong" from $\lambda 6101$ and $\lambda 6168$ absorption are classified as "weak" from $\lambda 5534$, $\lambda 5577$, and $\lambda 5625$ absorption. With this adjustment, we find that 19 of the 33 carbon stars show medium or strong $^{12}C^{13}C$. In column (9) of Table 2 we present the classifications for $^{12}C^{13}C$ and mark with a superscript "a" those stars whose $^{12}C^{13}C$ heads are highlighted in Figure 7. Based on these rough classifications we consider BW-2, BW-7, N6558-3, N6558-6, GWX 1-2, and GWX 1-6 to be the best ^{13}C -rich J-star candidates. Clear verification will require high-

resolution spectra near 4752 Å, where the C_2 isotopic band-heads are well separated and unblended.

Many bulge carbon stars have a dip in their continuum in the vicinity of 5900 Å. It is occasionally suggested that this feature is a general property of ^{13}C -rich stars (e.g., Lloyd Evans 1985). We find for the bulge carbon stars, however, that the dip is more a property of the overall strength of the C_2 Swan system than of the prevalence of carbon isotopes in the spectra. For example, N6558-5 and BW-8 each shows only weak $^{12}C^{13}C$ absorption, yet N6558-5 has one of the largest dips at 5900 Å with strong C_2 at $\lambda 5635$ and $\lambda 6060$ (see Fig. 8f), and BW-8 has one of the smallest dips around 5900 Å with weak C_2 at $\lambda 5635$ and $\lambda 6060$ (see Fig. 8b).

If these bulge carbon stars were in binary systems where the primary was a classical late N-type carbon star that had deposited its ^{12}C rich envelope to its less massive companion, then we would not expect to see strong $^{12}C^{13}C$. These N stars typically have $30 < ^{12}C/^{13}C < 70$ (Jaschek and Jaschek 1987; Lambert *et al.* 1986; Fujita and Tsuji 1977) while most of the bulge carbon stars appear to have a much lower $^{12}C/^{13}C$ ratio based on a visual comparison of BD + 332399 ($^{12}C/^{13}C = 5 \pm 4$; Dominy 1984) with the four representative bulge carbon stars in Figure 7. McClure (1985) also notes that early R stars (unlike the well-studied halo CH stars) have the same binary frequency as normal giants.

Enhanced ^{13}C in carbon star spectra, or more specifically a low $^{12}C/^{13}C$ ratio, is generally interpreted as the signature of the equilibrium products of the CN cycle of hydrogen burning. Isotopic carbon can be enhanced by convective cycling of envelope ^{12}C through a H-burning shell at $\sim 60 \times 10^6$ K. At this temperature ^{13}C is produced through $^{12}C(p, \gamma)^{13}N(\beta^+ \nu)^{13}C$.

It was emphasized by Harris *et al.* (1987) that to invoke the CN cycle to boost ^{13}C will also boost ^{14}N via $^{13}C(p, \gamma)^{14}N$ because the ^{13}C to ^{14}N reaction operates faster at all temperatures than the ^{12}C to ^{13}C reaction (Clayton 1983). In considering a sample of five J-stars, Harris *et al.* (1987) find that the CN cycle operating in equilibrium cannot reconcile the high ^{13}C abundances with the low ^{14}N abundances. If CN traces the nitrogen abundance, then we should expect the CN absorption to be higher for the ^{13}C strong and medium stars than for the ^{13}C weak stars. We investigated this effect in the bulge carbon stars and found, after removing the latitude dependence, that the mean CN absorption was slightly (1σ) higher in the ^{13}C strong and medium stars than in the ^{13}C weak stars. While this comparison is admittedly crude, it suggests that, at least for the bulge, we need not discount entirely the intermediate products of the CN cycle as the source for enhanced ^{13}C . We may also appeal to a scenario similar to Dominy (1984) where the ^{13}C formation occurs at the core helium flash. The fresh ^{12}C passes explosively through the hydrogen burning envelope and makes ^{13}C without significant losses to ^{14}N .

c) Panels

Figure 8 consists of eight panels that contain spectra of the 33 bulge carbon stars smoothed to 8 Å resolution. It has been shown that a blackbody fit is a good approximation to the broad-band energy distribution of carbon stars (Scalo 1976). The continuum maxima of all spectra suggest blackbody color temperatures between 4100 and 4800 K, which is consistent with the class of (nonvariable) early R stars (Scalo 1976; Dominy 1984). All spectra are in units of relative F_λ and are

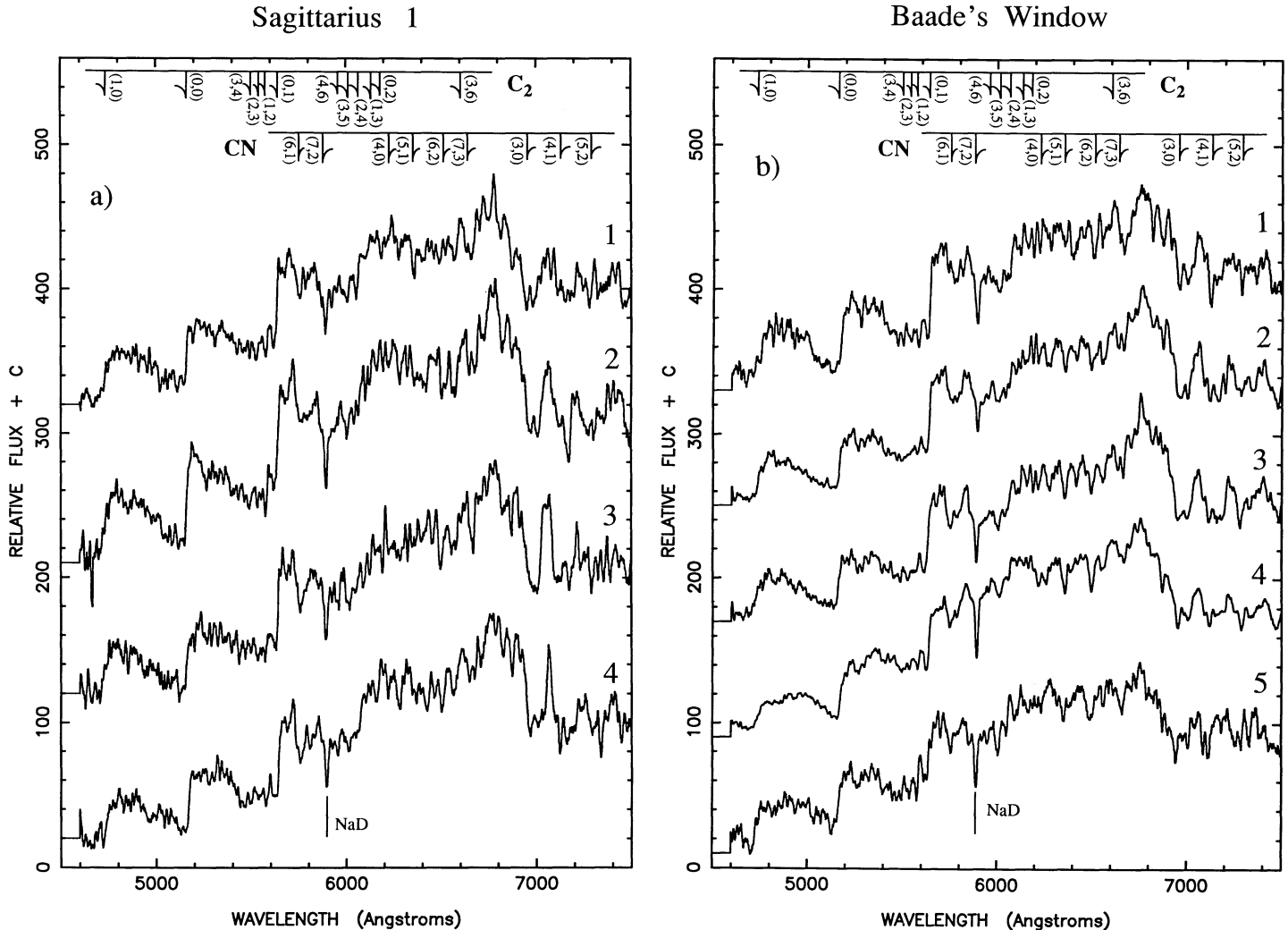


FIG. 8.—Spectra (smoothed to 8 Å resolution) of all 33 carbon stars appear in eight panels ([a]–[h]). Each panel is identified by the bulge window in which the carbon stars are found, while each spectrum is identified by an ordinal number assigned by Azzopardi *et al.* (1985). Absorption features of C₂ and CN dominate these optical spectra and are noted at the top of each panel. Stars that warrant individual discussion are detailed in § IVc. The flux standard G158-100 was used to convert all displayed spectra to a monochromatic flux scale.

scaled such that the continuum region between 6100 and 6500 Å is 100 flux units above the zero flux line segment at the left of each spectrum. Each panel is identified by its window name, while each spectrum is labeled with its ordinal number as designated by Azzopardi, Lequeux, and Rebeiro (1985). Several features are noted, including the characteristic C₂ Swan bands (shortward of λ4737, λ5165, λ5635, and λ6060), NaD, and CN bands longward of λ6900. Table 7 lists all related spectral features. Below we highlight for each panel those carbon stars that warrant closer attention.

Figure 8a.—The Sagittarius 1 window is the nearest to the Galactic center ($b = -2.7^\circ$). Its four carbon stars show strong CN absorption longward of λ6900. Sgr 1-3 has strong C₂, NaD, and CN absorption. A segment of its echelle spectrum, centered on the location of H α , is featured in Figure 9. We classify it, along with 12 other bulge carbon stars, as hydrogen-deficient. Sgr 1-4 has the strongest CN (3, 0) absorption of all 33 carbon stars.

Figure 8b, c.—Baade's window ($b \approx -4.0^\circ$) contains nine carbon stars that also show strong CN absorption longward of λ6900. The region from 6080 to 6300 Å is highlighted in Figure

7 for BW-2 where the ¹²C¹³C (λ6101, λ6168) isotope shifts are noted. The strength of these features suggests that BW-2 is a ¹³C-rich J-star.

Figure 8d.—Galactic window X2 (GWX 2; $b \approx -4.8^\circ$) contains six carbon stars. GWX 2-1 shows moderately strong ¹²C¹³C absorption at λ6101 and λ6168 which is highlighted in Figure 7. GWX 2-3 has weak Swan C₂ (0, 0; 0, 1) absorption presumably due to a C/O ratio near unity. It is one of two stars among the 33 that we consider to be a CS star candidate.

Figure 8e.—The Sagittarius 2 window ($b \approx -5.0^\circ$) contains two carbon stars. Aside from the CS stars, Sgr 2-1 has the weakest Swan C₂ (0, 0; 0, 1) absorption.

Figure 8f.—The N6558 window ($b \approx -6.0^\circ$) contains the carbon star N6558-5, which has pronounced $\Delta v = -2$ Swan absorption: C₂(4, 6), C₂(3, 5), C₂(2, 4), C₂(1, 3), and C₂(0, 2). This system appears to be responsible for the dip in the continuum around 5900 Å for most of these bulge carbon stars. N6558-5 shows only a weak presence of ¹²C¹³C and ¹³C¹⁴N, as seen in Figure 7 where N6558-4 is also highlighted.

Figure 8g.—Galactic window X1 (GWX 1; $b \approx -6.5^\circ$) contains four carbon stars. GWX 1-2 has the strongest Swan

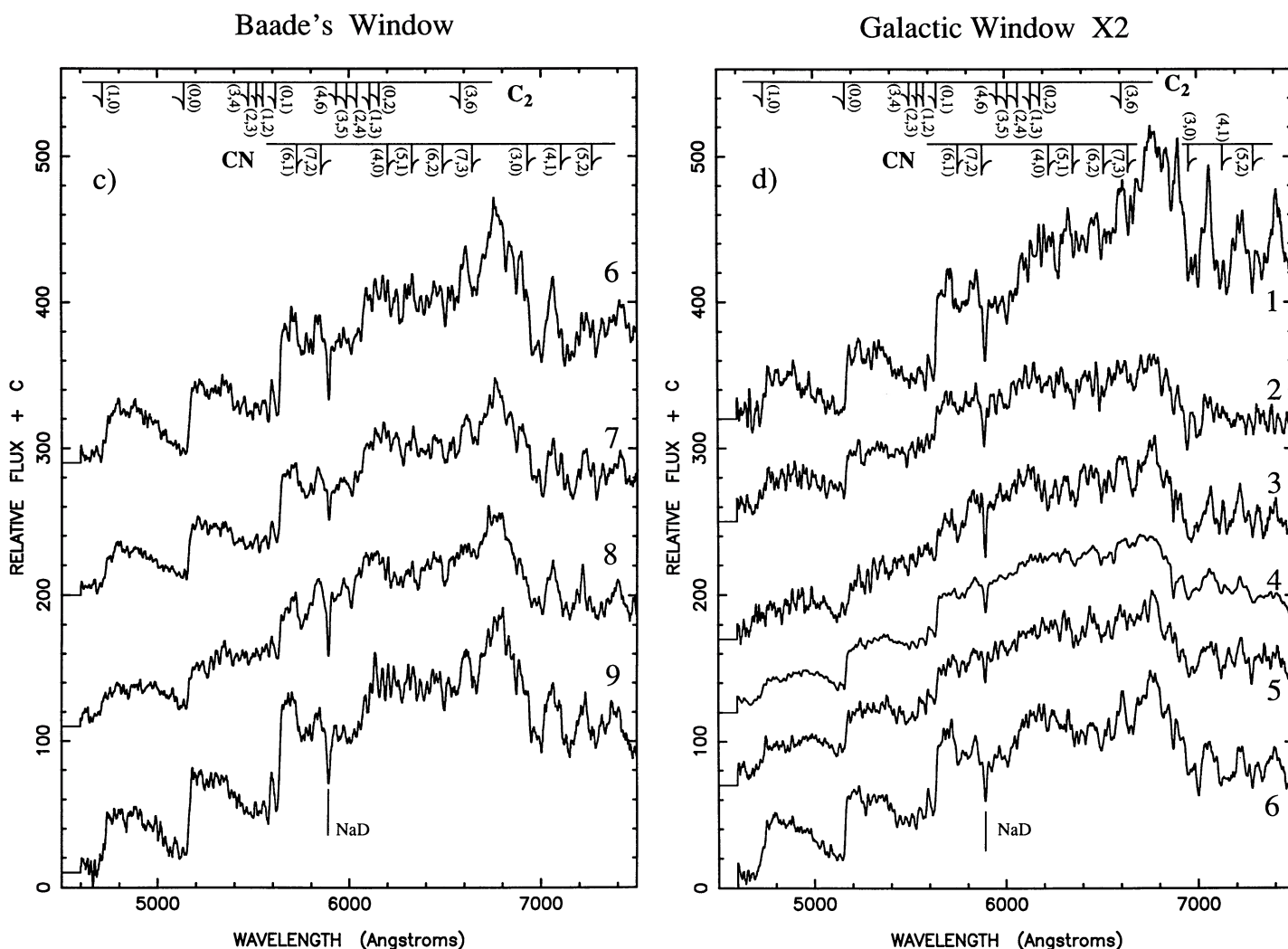


FIG. 8—Continued

$C_2(0, 0; 0, 1)$ system of all 33 carbon stars and a pronounced dip in the spectrum around 5900 Å, as noted previously for N6558-5: GWX 1-4 is a CS star as evidenced by its weak Swan bands. It also shows the anomalous enhancement of NaD ($EW = 8.2$ Å) expected when $C \approx O$ (Scalo 1973).

Figure 8h.—van den Bergh's window (VDB; $b \approx -8^\circ 0$) and Gröningen-Palomar 3 (GP 3; $b \approx -10^\circ 0$) each contains one carbon star. GP 3-1 is the farthest bulge carbon star in this sample from the Galactic center. It also displays the weakest absorption in NaD ($EW = 1.8$ Å). The third spectrum in Figure 8h is ROA 153, which served as the radial velocity template. Below it are the wavelength intervals used to fit the continuum and measure the band strengths of $C_2(0, 0)$, $C_2(0, 1)$, $Na[D_1 + D_2]$, $CN(3, 0)$, and $CN(4, 1)$ for the 33 stars.

Mass-loss from a carbon-rich atmosphere can form silicate dust shells as demonstrated for some of the ^{13}C enhanced local carbon stars discussed in Lloyd Evans (1990). The molecule SiC_2 is responsible for the prominent Merrill-Sanford absorption bands at 44640, 44866, 44905, 44977, and 45192. None of the bulge carbon stars, however, shows signs of this absorption. At 5 Å resolution, the bulge carbon stars also show no evidence of $Li\ I\ \lambda 6707$ enhancement. We note that if lithium were present, we might expect it to be anomalously enhanced

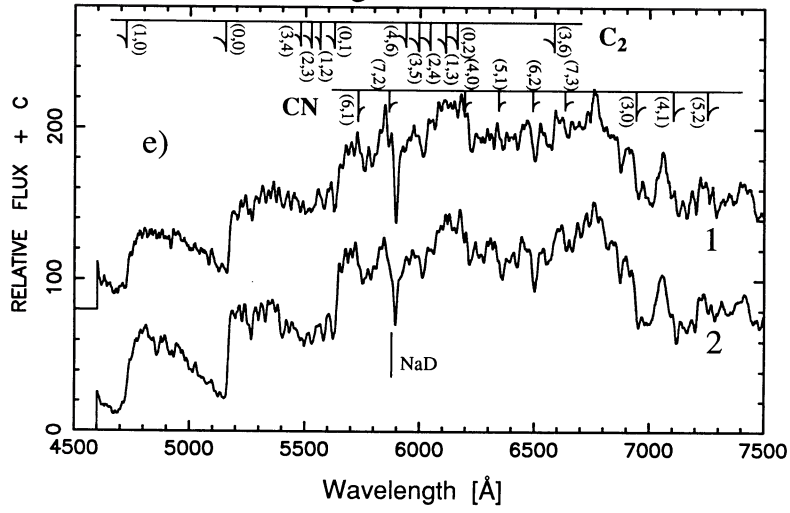
(along with NaD) in the CS star, GWX 1-4 (Scalo 1973). The bulge carbon stars also show no enhanced $Ba\ II\ \lambda 4934$ as is true with other early R stars. Barium and s -process enhancement in general are considered indicators of binary mass transfer, which has been invoked to explain the origin of barium and CH stars (McClure 1984).

V. DISCUSSION

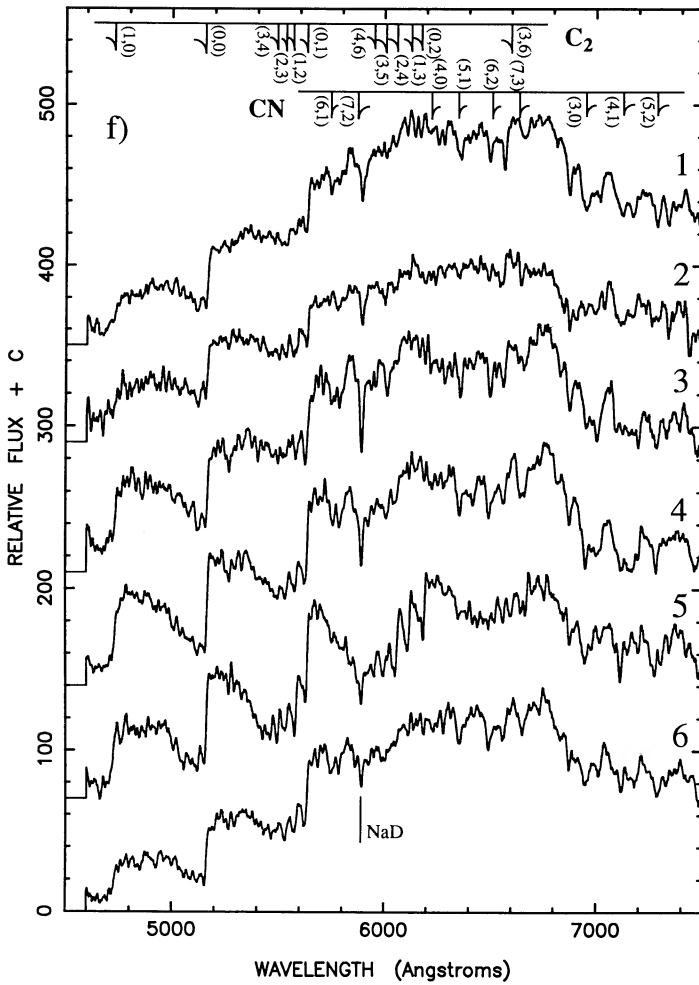
We characterize the bulge carbon stars as warm ($4100^\circ < T_{\text{eff}} < 4800^\circ$) and underluminous ($-2.5 < M_{\text{bol}} < 1$) like the classical early R stars. Nineteen out of 33 appear to have enhanced ^{13}C , and the 5 Å resolution spectra show no lithium or s -process enhancement. Twenty-six of the carbon stars display much stronger NaD and CN absorption than globular cluster and solar neighborhood counterparts. The high line strengths, perhaps indicative of high metallicity, are unexpected. While many of the bulge carbon stars are hydrogen-deficient, none has the SiC_2 absorption bands characteristic of recent carbon-rich mass loss.

In considering a scenario for the evolution of the bulge carbon stars, we are guided by their similarity to the early R stars. McClure (1985) finds that in contrast to the Ba and CH stars, early R stars in the field have a normal binary frequency.

Sagittarius 2



N6558



Galactic Window X1

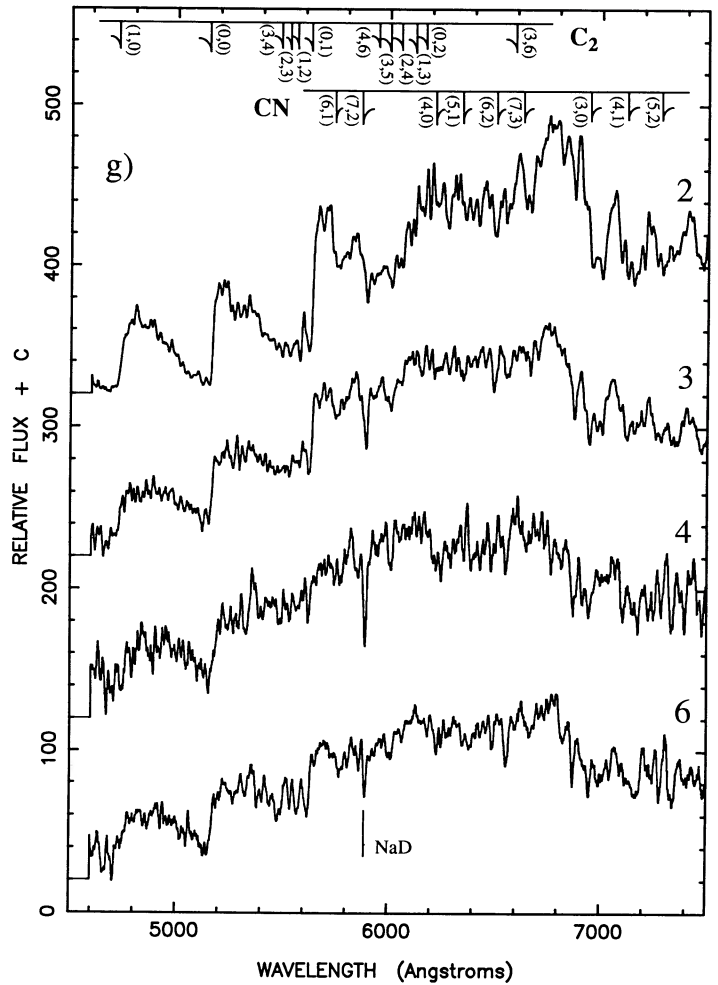


FIG. 8—Continued

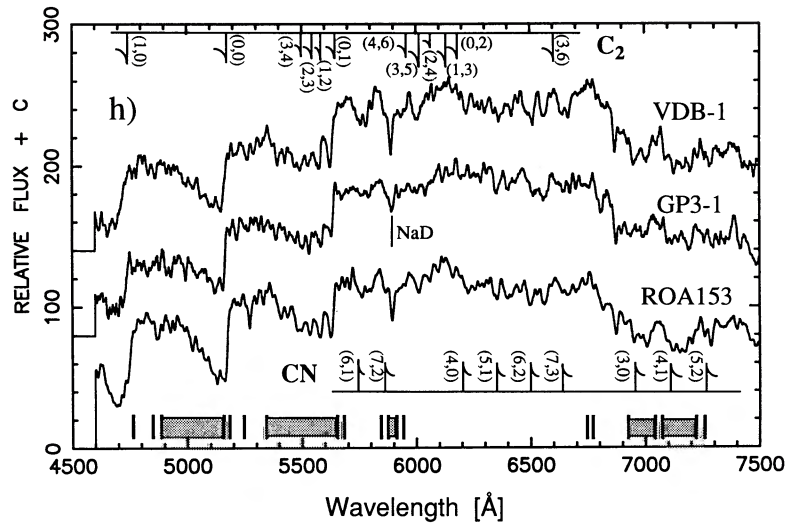


FIG. 8—Continued

A binary hypothesis involves the transfer of ^{12}C -rich material ($^{12}\text{C}/^{13}\text{C} > 30$) produced via 3α from a classical N-type carbon star. The material also contains s -process elements forged in the neutron-rich environment of the CNO cycle operating at high temperatures in the hydrogen-burning shell. The bulge carbon stars (as well as the early R stars) show strong ^{13}C ($^{13}\text{C}/^{12}\text{C} < 10$) and no s -process enhancement. These factors prompt us to consider single star evolutionary scenarios.

The inferred high metallicity for these bulge carbon stars is entirely unexpected. For a given C/O abundance ratio, a metal-rich star has a larger (O-C)/H than does a metal-poor star. Whatever process is responsible for raising the carbon

abundance to C/O > 1 must occur more times or more vigorously in a metal-rich star to create a carbon star. Consequently, at least for the cooler classical N and late R carbon stars, metal-poor environments contain more carbon stars relative to M giants than do metal-rich environments (Scalo and Miller 1981).

To reconcile these various carbon star properties, we suggest the following evolutionary scenario: we start with a low-mass star ($0.7 < M/M_{\odot} < 1.0$, core mass: $0.6 M_{\odot}$) that is metal-rich. After core hydrogen exhaustion, during its ascent of the red giant branch or at the core helium flash, it loses a significant fraction of its envelope mass. The lost outer hydrogen envelope has C/O < 1, which precludes the formation of SiC_2 since nearly all the carbon will have formed CO. The reduced mass of the star's envelope contains fewer oxygen atoms. Consequently, the difference between the number of oxygen atoms and the number of carbon atoms (O - C) becomes the same as that for a star with a metallicity that is lower by the same factor as the ratio of the remaining envelope mass to the mass of the original envelope. If, for example, 90% of the envelope mass is lost, then a $3 Z_{\odot}$ star will have the same O - C as a star with $0.3 Z_{\odot}$. The result is a weaker obstacle for carbon mixing to create a carbon star. Thus, it is possible to tip the balance from C/O < 1 to C/O > 1 even for a star of intrinsically high metallicity. This idea is supported by the fact that the mean equivalent width of the C_2 ($\Delta v = -1$; head at 5635 \AA) absorption complex is 50% larger in those stars (13 total) with weak or nonexistent $\text{H}\alpha$ absorption when compared with the rest of the sample (see Fig. 10).

Mass loss is a signature of AGB evolution where carbon-rich mass loss can be as common as oxygen-rich mass loss (Jura and Kleinmann 1989). Significant mass loss is not expected, however, on the first ascent of the giant branch, although it is well known that, based on evolutionary models, the masses of horizontal-branch stars in globular clusters are often found to be up to $0.3 M_{\odot}$ less than the turnoff mass (Renzini 1981; Iben and Rood 1970). The cause of this mass loss is still unclear. We emphasize that for most (eight of 13) of the bulge carbon stars classified as hydrogen deficient it is not clear whether they have any hydrogen at all at 5 \AA resolution. Carbon star spectral features are not uncommon among other stars classified as

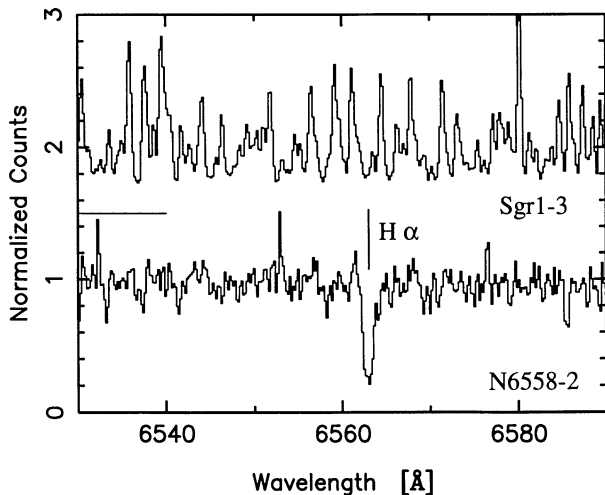


FIG. 9.—Subset of echelle spectra for two carbon bulge stars that highlights $\text{H}\alpha$ absorption. The very strong lined bulge carbon star, Sgr 1-3 ($S/N \approx 40$), shows no obvious presence of $\text{H}\alpha$ when compared with the bulge carbon star N6558-2 ($S/N \approx 20$). The continuum of N6558-2 is normalized to unity. For Sgr 1-3, the units are identical but the zero point is at 1.5, indicated by the solid line segment on the left-hand side of the figure. The absence of $\text{H}\alpha$ in 13 of the 33 bulge carbon stars may indicate for these stars an earlier episode (on the RGB or at the helium flash) where most of their hydrogen-rich envelope was lost. Such a scenario might assist carbon star formation for a high-metallicity star.

TABLE 7
SPECTRAL FEATURES

Species	Wavelength (Å)
SiC ₂	4640
C ₂ (1, 0)	4737.1
SiC ₂	4866
SiC ₂	4905
Ba II	4934.1
SiC ₂	4977
C ₂ (0, 0)	5165.2
SiC ₂	5192
C ₂ (3, 4)	5501.9
¹² C ¹³ C(2, 3)	5534
C ₂ (2, 3)	5540.7
¹² C ¹³ C(1, 2)	5577
C ₂ (1, 2)	5585.5
¹³ C ¹³ C(0, 1)	5615
¹² C ¹³ C(0, 1)	5625
C ₂ (0, 1)	5635.5
CN(6, 1)	5748.7
CN(7, 2)	5877.6
Na I(D ₁ , D ₂)	5890.0, 5895.9
C ₂ (4, 6)	5959.0
C ₂ (3, 5)	6004.8
C ₂ (2, 4)	6059.7
¹² C ¹³ C(1, 3)	6101
Ca I(3)	6103
Ca I(3)	6122
C ₂ (1, 3)	6122.2
Ca I(3)	6162
¹² C ¹³ C(0, 2)	6168
Ca I(20)	6169
C ₂ (0, 2)	6191.3
CN(4, 0)	6206.1
¹³ C ¹⁴ N(4, 0)	6259
CN(5, 1)	6355.1
CN(6, 2)	6502.3
Hα	6562.8
C ₂ (3, 6)	6599.1
CN(7, 3)	6656.6
Li I	6707
CN(3, 0)	6954.3
CN(4, 1)	7119
CN(5, 2)	7283

NOTE.—C₂ band heads from Pearse and Gaydon 1963 and Phillips and Davis 1968. ¹²C¹³C, and ¹³C¹³C, and ¹³C¹⁴N band heads from Sanford 1950. SiC₂ band heads from Lloyd Evans 1990. Ca I wavelengths from Mäcke *et al.* 1975*a, b*. CN band heads from Pearse and Gaydon 1963. Other wavelengths from Turnshek *et al.* 1985.

hydrogen deficient, such as the cool RCrB stars (Jaschek and Jaschek 1987) and the hot extreme helium stars (e.g., BD + 102179; Schönberner and Wolf 1974).

Thus far, we have described a scenario whereby a metal-rich star may become a candidate for carbon star status. To understand how carbon may rise to the surface of a warm, low-luminosity (non-AGB) star may require a closer look at the helium flash. With this in mind, Dominy (1984) proposes that fresh ¹²C from 3α is injected to the envelope at the helium flash which is followed by ¹³C enrichment through ¹²C(*p, γ*)¹³N(*β⁺ν*)¹³C at a temperature of less than 60 × 10⁶ K in a hydrogen-burning shell. At higher temperatures (~100 × 10⁶ K), the reaction ¹³C(*α, n*)¹⁶O will boost the oxygen abundance and provide a neutron source that would enhance the *s*-process elements in conflict with what is observed. The capability of the line-forming region to mix the

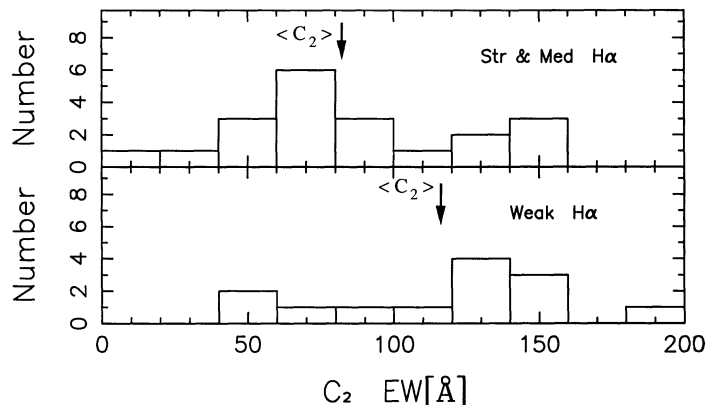


FIG. 10.—Distribution of C₂ equivalent widths for the 20 bulge carbon stars with strong to medium Hα (top histogram) and the 13 bulge carbon stars with weak Hα (bottom histogram). The mean C₂ equivalent width for those stars with weak Hα is 50% larger than the mean C₂ equivalent width for those stars with strong Hα.

fresh ¹²C and subsequent ¹³C may be enhanced by the deep convective envelope that we expect from the high opacity and steep temperature gradient within the envelope of a metal-rich star. With deep convection, we can also appeal to the “hot bottom” CN processing (Renzini and Voli 1981) to enhance ¹³C continuously. With such a scenario, we believe that a metal-rich star may become a carbon star as readily as one that is metal-poor.

While the proposed chain of events is nonstandard, we at least are not forced to appeal to an unknown, exotic process to produce a carbon-rich atmosphere. A distribution of mass loss among giant branch stars—where the bulge carbon stars are the high mass-loss tail—or the rarity of mixing at the He flash may explain why there are so few carbon stars in the bulge.

VI. SUMMARY

We present medium-resolution optical spectra of the 33 known carbon stars (discovered by Azzopardi, Lequeux, and Rebeiro 1985) in eight low-extinction windows to the Galactic bulge. From these spectra we obtain the radial velocity distribution and find the dispersion to be $113 \pm 14 \text{ km s}^{-1}$ and the mean to be $-44 \pm 20 \text{ km s}^{-1}$. The dispersion is consistent with that of the bulge K and M giants. The velocity dispersion of the carbon stars, when binned into three latitude zones, decreases from 131 km s^{-1} for the inner zone to 81 km s^{-1} for the outer zone. From the velocity distribution we find that the carbon stars do not share the kinematics of the local neighborhood and are likely to be genuine bulge members, thus permitting distances and accurate luminosities to be assigned. The mean velocity is significantly nonzero even though the stars are all near $l = 0^\circ$ and becomes increasingly negative at higher latitudes. Radial velocities of bulge stars at northern latitudes will be required before minor axis rotation can be established.

If the NaD and CN absorption primarily traces metallicity in this sample of warm (4100–4800 K) carbon stars, then the bulge exhibits a strong abundance gradient. We find that the NaD equivalent width increases with decreasing Galactic latitude even when we account for interstellar absorption. The CN band at $\lambda 6928$ is also correlated with Galactic latitude and is therefore correlated with NaD. Six of the bulge carbon stars share similar NaD and CN absorption to local early R stars (with solar Fe abundance) and the ω Cen CH stars. The remaining 27 bulge carbon stars form a separate group with

much stronger lines; it is possible that the stars with weaker lines may belong to a different population such as the inner halo.

Nineteen of the carbon stars show enhanced ^{13}C , six of which (BW-2, BW-7, N6558-3, N6558-6, GWX 1-2, and GWX 1-6) we consider to be J-star candidates. Two of the carbon stars (GWX 1-4 and GWX 2-3) show weak C_2 absorption, which classifies them as CS stars. The absence of barium and s-process elements in general (at 5 Å resolution) argues against a binary mass transfer mechanism as the origin of these low-luminosity carbon stars. Higher resolution spectra (< 1 Å) over several years to monitor radial velocities are necessary to establish the frequency of binaries of the sample. Thirteen carbon stars appear to be hydrogen-deficient based on the absence or weakness of H α absorption.

We propose that mass loss on the first giant branch or during the core helium flash may remove enough envelope mass (thus lowering O – C) to allow a metal-rich giant to

become a carbon star. It may be that the bulge carbon stars are rare, due to the large mass loss required and/or the infrequency with which carbon is mixed into the atmosphere at the core helium flash.

We thank M. Azzopardi for kindly providing excellent finding charts in advance of publication. We have enjoyed conversations with G. Wallerstein, V. Smith, R. Wing, J. Applegate, W. van der Veen, J. Frogel, and D. Terndrup. We also thank R. Gal for his assistance with parts of the data reduction. N. D. T. gratefully acknowledges the ARCS Foundation for partial support. R. M. R. thanks F. Peralta and A. Guerra, and H. Solis of the Las Campanas Observatory staff for their expert assistance with the observations and data system. R. M. R. acknowledges the Director of the Mount Wilson and Las Campanas Observatories for generous allocation of observing time in the 1986 season. This work is Contribution No. 452 of the Columbia Astrophysics Laboratory.

REFERENCES

- Azzopardi, M., Lequeux, J., and Rebeiro, E. 1985, *Astr. Ap.*, **145**, L4.
 ———. 1988, *Astr. Ap.*, **202**, L27.
 ———. 1991, in preparation.
 Blanco, V. M. 1986, *A.J.*, **91**, 290.
 ———. 1988, *A.J.*, **95**, 1400.
 Blanco, V. M., and Blanco, B. M. 1985, *Mem. Soc. Astr. Italiana*, **56**, 15.
 Blanco, V. M., McCarthy, M. F., and Blanco, B. M. 1984, *A.J.*, **89**, 636.
 Blanco, V. M., and Terndrup, D. 1989, *A.J.*, **98**, 843.
 Blitz, L., and Spergel, D. 1991, in press.
 Bond, H. E. 1975, *Ap. J. (Letters)*, **202**, L47.
 Clayton, D. D. 1983, *Principles of Stellar Evolution* (Chicago: University of Chicago Press).
 Dominy, J. F. 1984, *Ap. J. Suppl.*, **55**, 27.
 Fujita, Y., and Tsuji, T. 1977, *Pub. Astr. Soc. Japan*, **29**, 711.
 Gerhard, O. E., and Vietri, M. 1986, *M.N.R.A.S.*, **223**, 377.
 Gordon, C. P. 1971, *Pub. A.S.P.*, **83**, 667.
 Harris, M. J., Lambert, D. L., Hinkle, K. H., Gustafsson, B., and Eriksson, K. 1987, *Ap. J.*, **316**, 294.
 Horne, K. 1986, *Pub. A.S.P.*, **98**, 609.
 Iben, I. 1975, *Ap. J.*, **196**, 525.
 ———. 1983, *Ap. J. (Letters)*, **275**, L65.
 ———. 1984, in *IAU Symposium 105, Observational Tests of Stellar Evolution Theory*, ed. A. Maeder and A. Renzini (Dordrecht: Reidel), p. 3.
 Iben, I., and Renzini, A. 1982a, *Ap. J. (Letters)*, **263**, L23.
 ———. 1982b, *Ap. J. (Letters)*, **259**, L79.
 ———. 1983, *Ann. Rev. Astr. Ap.*, **21**, 271.
 Iben, I., and Rood, R. T. 1970, *Ap. J.*, **161**, 587.
 Jaschek, C., and Jaschek, M. 1987, *Classification of Stars* (Cambridge: Cambridge University Press).
 Jura, M., and Kleinmann, S. G. 1989, *Ap. J.*, **341**, 359.
 Lambert, D. L., Gustafsson, B., Eriksson, K., and Hinkle, K. H. 1986, *Ap. J. Suppl.*, **62**, 373.
 Lloyd Evans, T. 1985, *M.N.R.A.S.*, **216**, 3p.
 ———. 1990, *M.N.R.A.S.*, **243**, 336.
 Mäcke, R., Griffin, R., Griffin, R., and Holweger, H. 1975a, *Astr. Ap. Suppl.*, **19**, 303.
 Mäcke, R., Holweger, H., Griffin, R., and Griffin, R. 1975b, *Astr. Ap.*, **38**, 239.
 Maurice, E., et al. 1984, *Astr. Ap. Suppl.*, **57**, 275.
 McCarthy, J. 1988, Ph.D. thesis, Caltech.
 McClure, R. D. 1984, *Ap. J. (Letters)*, **280**, L31.
 ———. 1985, in *Cool Stars With Excess of Heavy Elements*, ed. M. Jaschek and P. C. Keenan (Dordrecht: Reidel), p. 315.
 Mould, J. R. 1983, *Ap. J.*, **266**, 255.
 Pearse, R. W. B., and Gaydon, A. G. 1963, *The Identification of Molecular Spectra* (New York: J. Wiley & Sons).
 Phillips, J. G., and Davis, S. P. 1968, *The Swan System of the C₂ Molecule* (Berkeley: University of California Press).
 Renzini, A. 1981, in *Effects of Mass Loss on Stellar Evolution*, ed. C. Chiosi and R. Stalio (Dordrecht: Reidel), p. 319.
 Renzini, A., and Voli, M. 1981, *Astr. Ap.*, **94**, 175.
 Rich, R. M. 1986, Ph.D. thesis, Caltech.
 ———. 1988, *A.J.*, **95**, 828.
 ———. 1989, in *The Center of the Galaxy* (Dordrecht: Reidel), p. 63.
 ———. 1990, *A.J.*, in press.
 Rich, R. M., and Tyson, N. D. 1991, in preparation.
 Rodgers, A. W. 1977, *Ap. J.*, **212**, 117.
 Sanduleak, N., and Philip, A. G. D. 1977, *Pub. Warner and Swasey Obs.*, **2**, 105.
 Sanford, R. F. 1950, *Ap. J.*, **111**, 262.
 Scalo, J. M. 1973, *Ap. J.*, **186**, 967.
 ———. 1976, *Ap. J.*, **206**, 474.
 Scalo, J. M., and Miller, G. E. 1981, *Ap. J. (Letters)*, **248**, L65.
 Shectman, S., and Hiltner, W. A. 1976, *Pub. A.S.P.*, **88**, 960.
 Schönberner, D., and Wolf, R. E. A. 1974, *Astr. Ap.*, **37**, 87.
 Terndrup, D. M. 1988, *A.J.*, **96**, 844.
 Terndrup, D., Frogel, J., and Whitford, A. E. 1990, *Ap. J.*, **357**, 453.
 Tonry, J., and Davis, M. 1979, *Ap. J.*, **84**, 1511.
 Topaktas, L. 1981, *Astr. Ap. Suppl.*, **46**, 93.
 Turnshek, D. E., Turnshek, D. A., Crane, E. R., and Boeshaar, P. C. 1985, *An Atlas of Digital Spectra of Cool Stars* (Tucson: Western Research Company).
 Utsumi, K. 1987, in *Atmospheric Diagnostics of Stellar Evolution: Chemical Peculiarities, Mass Loss, and Explosion*, ed. K. Nomoto (Berlin: Springer), p. 44.
 van den Bergh, S., and Herbst, E. 1974, *A.J.*, **79**, 603.
 Webbink, R. 1981, *Ap. J. Suppl.*, **45**, 259.
 Whitford, A. E., and Rich, R. M. 1983, *Ap. J.*, **274**, 723.
 Wing, R. F., and Stock, J. 1973, *Ap. J.*, **186**, 979.

NEIL D. TYSON: Department of Astronomy, Pupin Physics Laboratories, Columbia University, New York, NY 10027

R. MICHAEL RICH: Department of Astronomy, Pupin Physics Laboratories, Box 1325, Columbia University, New York, NY 10027